Microsc. Microanal. 14, 571–580, 2008
doi:10.1017/S1431927608080963

Microscopy AND Microanalysis

On the Field Evaporation Behavior of a Model Ni-Al-Cr Superalloy Studied by Picosecond Pulsed-Laser Atom-Probe Tomography

Yang Zhou,[1] Christopher Booth-Morrison,[1] and David N. Seidman[1,2,*]

[1]*Department of Materials Science and Engineering, Northwestern University, 2220 Campus Drive, Evanston, IL 60208-3108, USA*
[2]*Northwestern University Center for Atom-Probe Tomography (NUCAPT), 2220 Campus Drive, Evanston, IL 60208-3108, USA*

Abstract: The effects of varying the pulse energy of a picosecond laser used in the pulsed-laser atom-probe (PLAP) tomography of an as-quenched Ni-6.5 Al-9.5 Cr at.% alloy are assessed based on the quality of the mass spectra and the compositional accuracy of the technique. Compared to pulsed-voltage atom-probe tomography, PLAP tomography improves mass resolving power, decreases noise levels, and improves compositional accuracy. Experimental evidence suggests that Ni^{2+}, Al^{2+}, and Cr^{2+} ions are formed primarily by a thermally activated evaporation process, and not by post-ionization of the ions in the 1^+ charge state. An analysis of the detected noise levels reveals that for properly chosen instrument parameters, there is no significant steady-state heating of the Ni-6.5 Al-9.5 Cr at.% tips during PLAP tomography.

Key words: pulsed-laser atom-probe tomography, post-ionization, preferential evaporation, nickel-based superalloys

Introduction

Pulsed-laser atom-probe (PLAP) tomography permits atom-probe tomography (APT) with increased mass resolving power and pulse repetition rate, and allows the study of materials with poor electrical conductivity (Tsong, 1978; Kellogg & Tsong, 1980; Kellogg, 1987). PLAP tomography extends the range of study of the APT technique, though there are some inherent drawbacks, such as inaccurate quantitative results that can arise due to the complexity of the evaporation mechanism (Smith et al., 1982). Additionally, surface diffusion can occur if heating of samples is excessive under laser illumination. PLAP tomography has become an increasingly popular technique for the study of metals and semiconductors (Larson et al., 2004; Cerezo et al., 2007*a*; Gault et al., 2007*a*; Kelly et al., 2007; Kelly & Miller, 2007), thus a quantitative understanding of the effects of pico- or femtosecond laser pulsing on the evaporation behavior of investigated materials is essential to obtain physically meaningful results.

The extant theories of field evaporation, the image hump theory (Müller, 1956), and the charge exchange theory (Gomer, 1959, 1961; Gomer & Swanson, 1963) were successful in predicting both the correct charge state of evaporating atomic species and the electric fields required for evaporation, though refinement was required (Brandon, 1966*a*; Tsong, 1978). The ionic model upon which these theories are based treats the temperature dependence of the evaporation field to be exclusively from the heat of sublimation, which, from Kirchhoff's equation, displays very little temperature dependence from absolute zero to the melting point of metals (Zemansky, 1957). Hence, the ionic model is incapable of explaining the observed experimental temperature dependencies of the evaporation field, as the calculated values of the evaporation field in the literature are essentially 0 K values. While no fully satisfactory theoretical treatment of field evaporation is currently available (Miller & Smith, 1989; Tsong, 1990), modification of the image hump theory of field evaporation led to an expression for the temperature sensitivity of the evaporation field at constant evaporation rate (Brandon, 1964, 1965, 1966*a*). Brandon predicted an increase in the rate of evaporation with increasing temperature—predictions that were validated experimentally (Brandon, 1966*a*; Southon, 1968; Tsong & Müller, 1970; Ernst, 1979; Kellogg, 1981*a*, 1982; Wada, 1984; Miller & Smith, 1989). Currently, the mechanism by which laser pulsing induces field evaporation remains somewhat controversial, particularly for femtosecond laser pulsing (Cerezo et al., 2006, 2007*b*; Vella et al., 2006; Vurpillot et al., 2006; Bunton et al., 2007; Gault et al., 2007*b*). We note that

Received February 8, 2008; accepted August 18, 2008
*Corresponding author. E-mail: d-seidman@northwestern.edu

there is convincing evidence of heating of the tip under laser illumination with picosecond pulsing in other fields, such as scanning tunneling electron microscopy (Gerstner et al., 2000; Grafstrom, 2002). The theoretical and experimental work performed to measure the temperature rise due to laser illumination in field-ion microscopy has been reviewed in detail (Miller et al., 1996), though more work remains to be done, particularly for the new generation of atom probes using pico- and femtosecond laser pulsing.

In pulsed-voltage APT, variables such as sample preparation, instrument specifications, and the instrumentation parameters selected to evaporate ions, contribute to the quality of the data collected. Material- and specimen-dependent parameters, such as the evaporation behavior of the phases being studied and the crystallographic direction being examined, are also of critical importance and must be considered on a material-by-material basis. With the continued improvement in both instrument capability and sample preparation techniques (Bunton et al., 2007; Cerezo et al., 2007*a*; Kelly & Miller, 2007; Seidman, 2007*a*, 2007*b*), optimization of data quality must be performed by fine-tuning the instrumentation parameters, specifically (1) the specimen base temperature; (2) the pulse fraction, the ratio of the pulse voltage to the steady-state voltage; (3) the specimen evaporation rate, the number of ions evaporated per pulse; and (4) the pulse repetition rate. This has been performed extensively for pulsed-voltage atom-probe microscopy; see, for example, Yamamoto & Seidman, 1982, 1983; Herschitz & Seidman, 1983, who used a time-of-flight atom-probe field-ion microscope (Hall et al., 1977). Little, however, has been published on the quantification of the effects of the controllable experimental parameters in PLAP tomography (Smith et al., 1982), particularly for the new generation of high-performance instruments employing ultrafast pico- or femtosecond lasers. The instrumentation parameters for PLAP tomography are the same as those for pulsed-voltage APT, though the pulse fraction is replaced by the effective pulse fraction, which is not a directly tunable instrumentation parameter. The effective pulse fraction is defined as one minus the ratio of the steady-state tip voltage during laser-assisted data acquisition to the steady-state dc tip voltage required to field evaporate ions from a specimen at a rate of 10^3 ions per second (Bunton et al., 2007). The laser adds a further degree of complexity by introducing instrumentation variables such as the laser pulse energy, spot diameter, wavelength, and pulse widths. In the case of the LEAP 3000X Si™ instrument used in this study, these variables have been set by the instrument manufacturers (Bunton et al., 2007), with the exception of the laser pulse energy, which remains a variable instrumentation parameter under the control of the experimentalist.

It has been demonstrated that decreasing the laser pulse repetition rate and increasing the shank angle of specimen tips improves mass resolving power, $m/\Delta m$, the signal-to-noise ratio, S/N, and the compositional accuracy of PLAP tomography for materials with small values of the thermal diffusivity (Bunton et al., 2007; Cerezo et al., 2007*b*); the thermal diffusivity is equal to the ratio of the thermal conductivity to the product of the density and the specific heat at constant pressure. Little work has been performed to model the field evaporation of atoms in concentrated alloys because the relevant thermodynamic quantities are generally unknown (Miller & Smith, 1989), though some pioneering work was performed to model the field evaporation of solute atoms in dilute alloys of iron (Brandon, 1966*b*). The present study determines the effects of the laser pulse energy on the evaporation behavior of a concentrated model Ni-Al-Cr superalloy. The quality of the mass spectra and the compositional accuracy obtained for the same specimen, with varying picosecond pulse energies, are compared at constant base specimen temperature. These results are compared with those of a test of the effect of specimen base temperature on the evaporation behavior of the Ni-Al-Cr alloy, conducted by performing pulsed-voltage APT at different tip temperatures.

Materials and Methods

Ni-6.5 Al-9.5 Cr at.% solid solutions were homogenized at 1573 K for 20 h, solutionized at 1123 K for 3 h then water quenched to room temperature. The as-quenched solid solutions did not contain γ'-precipitates, and the chemical composition of the as-quenched samples was measured by inductively coupled plasma (ICP) atomic-emission spectroscopy to be Ni-6.24 Al-9.64 Cr at.%. Pulsed-laser and pulsed-voltage APT were performed employing an Imago Scientific Instrument's local-electrode atom-probe (LEAP™) tomograph (Bajikar et al., 1996; Kelly et al., 1996; Kelly & Larson, 2000), and APT data were analyzed employing the IVAS® 3.0 software program (Imago Scientific Instruments, Madison, WI, USA).

The data presented herein are obtained from two Ni-6.5 Al-9.5 Cr at.% tips: the first was analyzed by PLAP tomography to study the effects of the laser pulse energy, while the second tip was analyzed by pulsed-voltage APT to study the effects of specimen base temperature on the evaporation behavior of the Ni-Al-Cr alloy. Datasets of ~5 million atoms were collected for each laser pulse energy and specimen base temperature studied, and the first 0.5 million atoms were discarded due to the initial instability of evaporation upon application of the pulsed-laser or pulsed-voltage source. The depth of analysis of the datasets collected by pulsed-laser APT was constant at 21 ± 3 nm, with cross-sectional areas of 3,800 ± 300 nm^2, as determined by calculations based on the theoretical density of this alloy, with the tip radius estimated from the evaporation field of pure Ni at 73 K. PLAP tomography was performed at a constant specimen base temperature of 40 ± 0.3 K and ambient pressure of $<6.7 \times 10^{-8}$ Pa, a pulse repetition rate of 200 kHz, a specimen evaporation rate of 0.04 ions per

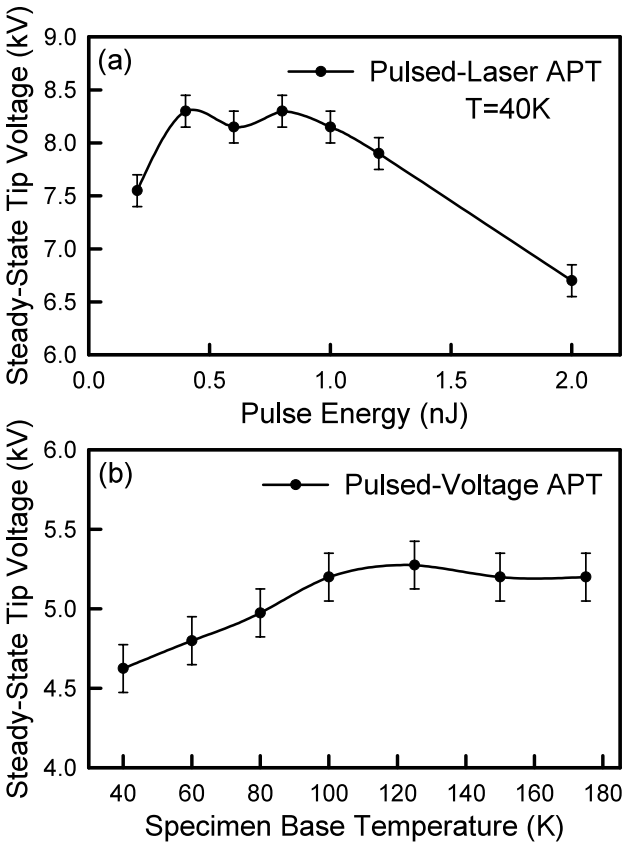

Figure 1. The steady-state dc voltage applied to the tip to maintain a specimen evaporation rate of 0.04 ions per pulse for a Ni-6.5 Al-9.5 Cr at.% alloy is shown as a function of (**a**) the laser pulse energy applied in PLAP tomography at a specimen base temperature of 40 ± 0.3 K and a pulse repetition rate of 200 kHz, and (**b**) the specimen base temperature used in pulsed-voltage APT at a pulse repetition rate of 200 kHz and a pulse fraction of ~20%.

pulse, and laser energies of 0.2, 0.4, 0.6, 0.8, 1.0, 1.2, or 2.0 nJ. A laser with a wavelength of 532 nm, a pulse duration of ~12 ps was used. Pulsed-voltage APT at a specimen base temperature of 40 ± 0.3 K was performed after the PLAP tomography runs at laser pulse energies of 0.6, 1.0, or 2.0 nJ to study the cumulative long-range effects of laser pulsing on the alloy composition.

Pulsed-voltage APT of a second tip was performed at a constant background pressure of $<6.7 \times 10^{-8}$ Pa, a pulse repetition rate of 200 kHz, a voltage pulse fraction (pulse voltage/steady-state DC voltage) of ~19%, a constant evaporation rate of 0.04 ions per pulse, and specimen base temperatures of 40, 60, 80, 100, 125, 150, or 175 ± 0.3 K. The depth of analysis of the datasets collected by pulsed-voltage APT was constant at 27 ± 2 nm, with cross-sectional areas of 2,200 ± 200 nm^2, as determined above. The steady-state tip voltages required to achieve a specimen evaporation rate of 0.04 ions per pulse for both pulsed-laser or pulsed-voltage APT are shown in Figure 1. We note that the tips had different initial radii of curvature and taper angles, and hence, under the same field evaporation conditions, the specimens required different steady-state voltages to evaporate atoms at the same rate. As such, results from the two Ni-Al-Cr tips studied herein are not comparable in a quantitative manner, though trends in the evaporation behavior provide insights into the effects of the picosecond laser pulse energy. The differences in the tip shapes and dimensions were such that the evaporation rates of the two tips differed when normalized to the effective area subtended by the detector. Normalized evaporation rates of $1.1 \pm 0.1 \times 10^{-5}$ ions $pulse^{-1}$ nm^{-2} and $1.8 \pm 0.2 \times 10^{-5}$ ions $pulse^{-1}$ nm^{-2} were achieved for pulsed-laser and pulsed-voltage APT, respectively.

Ni-Al-Cr samples in the as-quenched state were studied to avoid $\gamma'(L1_2)$-precipitation due to the problems associated with differences in the evaporation fields of the atomic species in the γ(face centered cubic)-matrix and γ'-precipitate phases. *No* γ'-precipitates are detected in the APT reconstructions, though partial radial distribution functions (Sudbrack et al., 2006*a*) of the as-quenched samples indicate small Ni-Al ordered domains, which evolve into γ'-precipitates upon subsequent aging. We note that deconvolution of the overlapping $^{27}Al^{1+}$ and $^{54}Cr^{2+}$ peaks was performed based on the relative abundances of Cr isotopes. The standard errors, 2σ, for all quantities are calculated based on counting statistics and reconstruction scaling errors, using standard error propagation methods (Parratt, 1966), and represent two standard deviations from the mean.

Results and Discussion

Mass Spectra

Figure 2 shows a comparison of the mass spectra obtained by PLAP tomography with laser energies of (a) 0.2 nJ per pulse and a steady-state tip voltage of 7.40–7.70 kV, (b) 1.0 nJ per pulse and a tip voltage of 8.0–8.3 kV, and (c) 2.0 nJ per pulse and a tip voltage of 6.55–6.85 kV. The amount of noise increases with increasing laser pulse energy; the percentage of evaporation events that are detected in expected ranges decreases from 97.24% at 0.2 nJ, to 95.15% at 1.0 nJ, to 93.96% at 2.0 nJ. We note that at a laser pulse energy of 2.0 nJ, the mass-to-charge state, m/n, spectrum is populated by numerous metal hydride peaks, particularly Ni^{1+} hydrides, and unexpected peaks at m/n ratios that correspond to hydrides, oxides, and metal ion clusters, which are probably a result of overheating of the tip. Because these peaks affect the quality of the compositional data obtained by PLAP tomography, laser energies greater than 1.0 nJ per pulse should be avoided for this alloy to minimize background noise and undesirable peaks. A section of the m/n range displaying the Ni^{2+} peaks is presented in Figure 3, to highlight both the improved $m/\Delta m$ values of PLAP tomog-

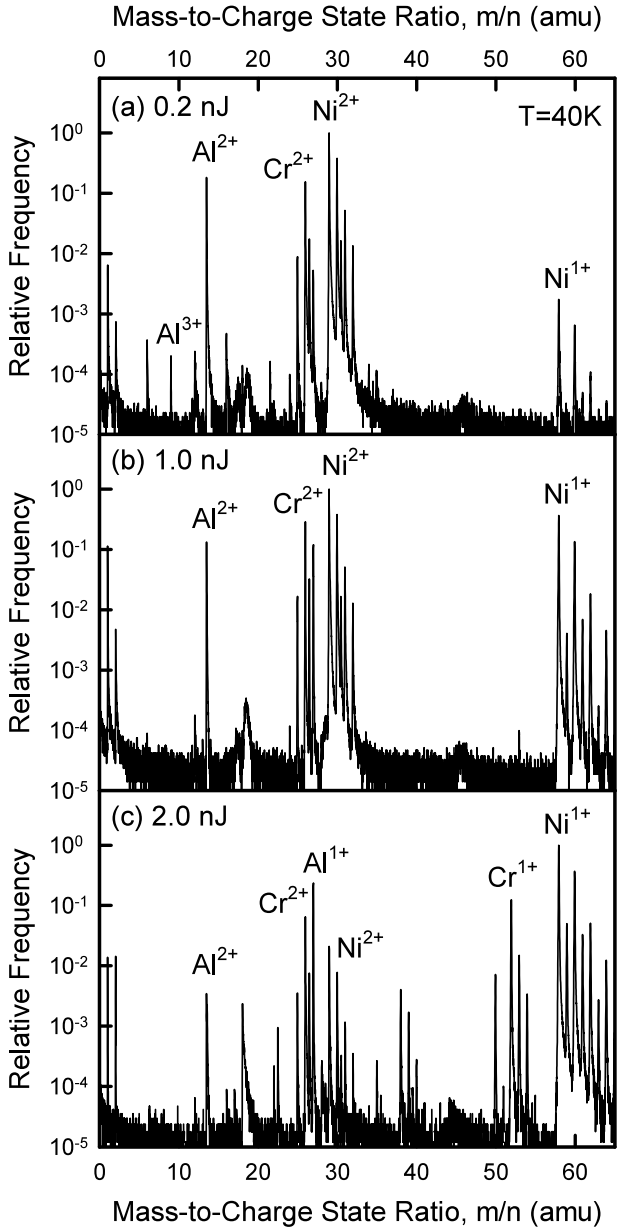

Figure 2. A comparison of the mass spectra obtained by PLAP tomography with laser pulse energies of (**a**) 0.2 nJ per pulse at a tip voltage of 7.40–7.70 kV, (**b**) 1.0 nJ per pulse at a tip voltage of 8.0–8.3 kV, and (**c**) 2.0 nJ per pulse at a tip voltage of 6.55–6.85 kV. The frequencies of detected events are normalized to the number of events detected in the most populous *m*/*n* bin. The *m*/*n* ratios of the evaporating species change by over four orders of magnitude with increasing laser pulse energy. At a laser pulse energy of 2.0 nJ per pulse, the *m*/*n* spectrum is populated by numerous hydrides, oxides, and metal ion clusters peaks, which are a result of overheating and are undesirable.

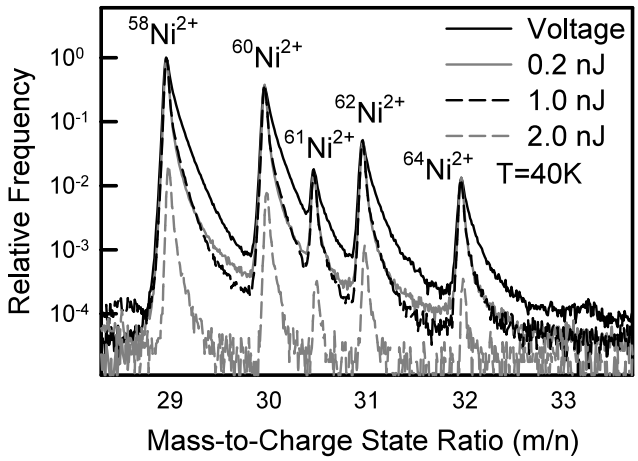

Figure 3. A section of the *m*/*n* range showing the Ni^{2+} peaks, highlighting both the improved mass resolving power of PLAP tomography when compared to pulsed-voltage APT, and the improved mass resolving power with increasing laser pulse energy. The relative frequencies of the Ni^{2+} peaks from the data set collected at a laser pulse energy of 2.0 nJ per pulse are nearly two orders of magnitude smaller than the relative frequencies of the Ni^{2+} peaks from the set collected at 0.2 nJ per pulse.

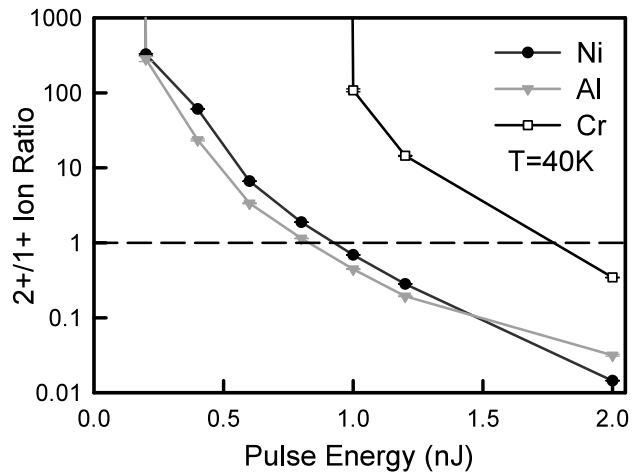

Figure 4. The ratio of the ions detected in the 2+ charge state to those detected in the 1+ charge state, as a function of laser pulse energy. The Ni and Al ions appear to have similar evaporation behavior, whereas Cr atoms evaporate exclusively as Cr^{2+} until the laser energy reaches 1.0 nJ per pulse.

raphy when compared to pulsed-voltage APT, and the improved $m/\Delta m$ values at higher laser pulse energies.

The most striking feature of Figures 2 and 3 is the dramatic change in the *m*/*n* ratios of the evaporating species with increasing laser pulse energy. The relative frequencies of the Ni^{2+} peaks from the data set collected at a laser energy of 2.0 nJ per pulse (Fig. 3) are nearly two orders of magnitude less than the relative frequencies of the Ni^{2+} peaks at 0.2 nJ per pulse. The Ni atoms are observed to evaporate as Ni^{1+} ions with increasing regularity as the laser pulse energy is increased. This trend is observed to hold for all the atomic species to varying degrees (Fig. 4). While Ni

and Al have similar evaporation behavior in terms of the m/n ratio, Cr evaporates exclusively as Cr^{2+} until the laser energy reaches 1.0 nJ per pulse, at which point the trend of the Cr^{2+}/Cr^{1+} ratio with increasing laser pulse energy is similar to that of Ni^{2+}/Ni^{1+} and Al^{2+}/Al^{1+}. Similar trends have been observed previously for other materials such as pure W, Si, Ni, Rh, Mo, Re, Ir, and Pt (Kellogg, 1981*b*, 1982, 1987; Cerezo et al., 2007*b*). High charge states on the order of 5+ and 6+ were detected for 5d transition metals evaporated at very high electric fields (Müller & Krishnaswamy, 1976).

It was previously suggested that field evaporated ions with lower than predicted m/n ratios were a result of post-ionization of desorbed ions by an electron tunneling mechanism similar to that involved in field ionization of gas atoms above the surface of the tip (Müller & Tsong, 1969; Forbes, 1976; Nakamura & Kuroda, 1977; Haydock & Kingham, 1980; Kingham, 1982). It was reasoned that the increased electric field required to maintain a constant evaporation rate at smaller laser pulse energies led to progressively more post-ionization of atoms, and to the appearance of lower m/n ratios. In Kellogg's PLAP tomography experiment with tungsten, for example, the ions field evaporated predominantly as W^{3+} at voltages greater than 3.6 kV, while they evaporated as predominantly W^{2+} at voltages less than 2.9 kV (Kellogg, 1981*b*). For the Ni-Al-Cr alloy studied here, when the laser pulse energy is varied between 0.4 and 1.0 nJ, the Ni^{2+}/Ni^{1+} and Al^{2+}/Al^{1+} ratios both decrease by more than two orders of magnitude. Over this range of laser pulse energies, the tip voltage required to maintain an evaporation rate of 0.04 ions per pulse only varies between 8.15 and 8.30 kV. Given that the applied electric field varies by no more than 2% over this range of laser energies, it is difficult to ascribe the dramatic changes in the charge state ratios exclusively to post-ionization. Additionally, if post-ionization is responsible for the higher charge states, the conditions required to post-ionize Ni^{1+} and an Al^{1+} ions differ significantly from those required to post-ionize Cr^{1+}. Thus, it may be that post-ionization is not solely responsible for the change in the charge state of the evaporated species in the Ni-Al-Cr alloy. We note that the average depth of the datasets was 21 ± 3 nm, thus the change in the radius of curvature, which affects the local electric field at the tip surface, is not responsible for a decrease in the ratio of the Ni^{2+}/Ni^{1+} and Al^{2+}/Al^{1+} of more than four orders of magnitude over the range of pulse energies studied herein.

Previous work with PLAP tomography at constant steady-state tip voltage and varying specimen base temperatures showed that temperature had *no* effect on the m/n ratio of evaporating species (Kellogg, 1981*b*, 1982). These results were interpreted to mean that the activation energies of desorption for ions of different charge states are identical and thus provided evidence for the post-ionization model. To quantify the importance of post-ionization in our model ternary alloy, a test at a constant specimen evaporation rate of 0.04 ions per pulse and varying specimen base temperature was performed for a second Ni-6.5 Al-9.5 Cr at.% tip to understand the effect of specimen base temperature on the evaporation behavior of this model Ni-Al-Cr alloy. The mass spectra from pulsed-voltage APT for specimen base temperatures ranging from 40–125 $\pm$ 0.3 K do not exhibit any evidence of evaporation of any of the atomic species in the 1^+ charge state. At specimen base temperatures of 150 and 175 $\pm$ 0.3 K, however, when the tip voltage is a constant 5.2 $\pm$ 0.2 kV, Ni^{1+} ions are detected and increase in relative frequency of occurrence with increasing temperature (Fig. 5). Thus, Ni atoms at specimen base temperatures below 150 K seem to field evaporate as Ni^{2+} ions and do not result from post-ionization of Ni^{1+} ions. For the evaporation conditions employed herein, Ni^{1+} ions field evaporate by a thermally activated process at temperatures of ~150 K and greater. Neither Al^{1+} nor Cr^{1+} ions are detected by pulsed-voltage APT, suggesting that, for the given evaporation conditions, the base specimen temperatures chosen herein are insufficient for evaporation of these ionic charge states. From these results, the change in the abundances of the charge states with increasing laser pulse energy in PLAP tomography (Fig. 4) *may* be partly or completely due to thermally activated field evaporation of ions in the 1^+ charge state at the higher tip temperatures that result from laser illumination.

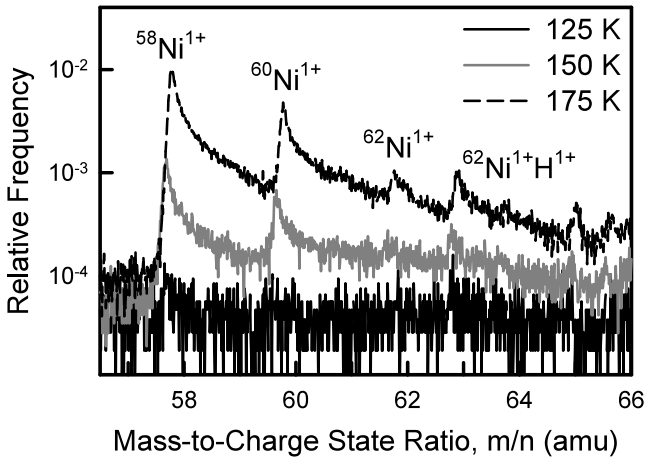

Figure 5. The relative frequencies of the Ni^{1+} peaks at specimen base temperatures of 125, 150, and 175 $\pm$ 0.3 K, at a constant steady-state dc tip voltage of 5.2 $\pm$ 0.2 kV. The increase in the relative frequency of Ni^{1+} ions with increasing specimen base temperature suggests that the evaporation of Ni^{1+} ions occurs by a different thermally activated mechanism than the evaporation of Ni^{2+} ions.

Compositional Accuracy: Effects of Laser Energy

The concentrations of Ni, Al, and Cr measured by PLAP tomography as a function of laser pulse energy are presented in Figure 6 and clearly demonstrate that the measured composition of the alloy differs with increasing laser

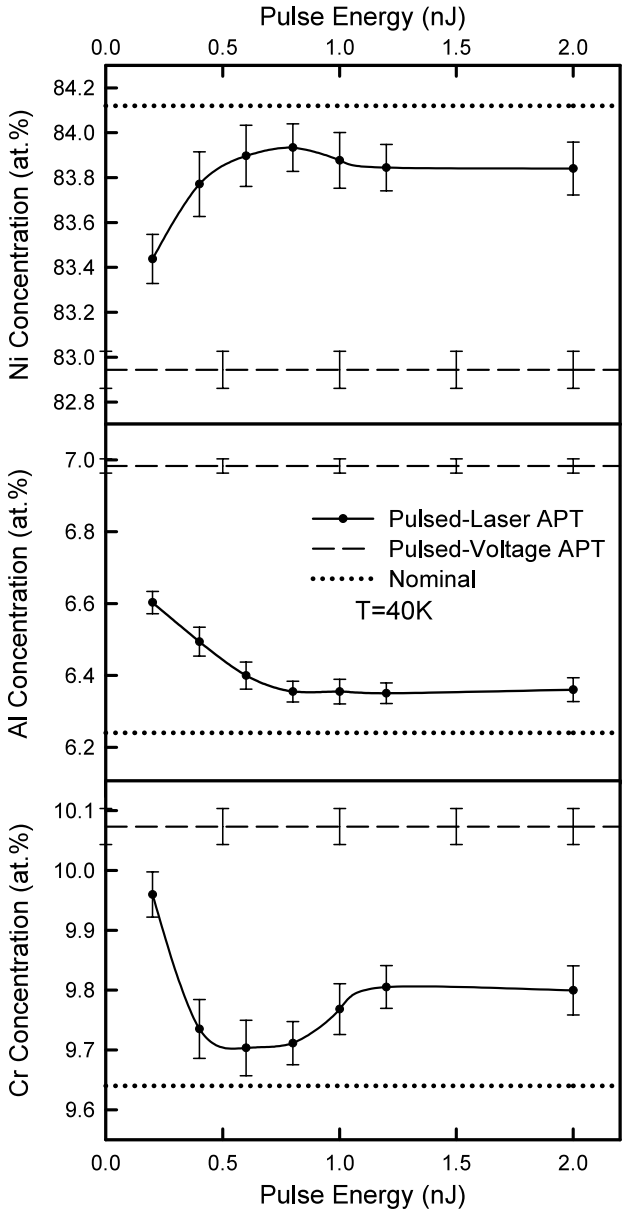

Figure 6. Variation in the detected composition of as-quenched Ni-6.5 Al-9.5 Cr at.% as a function of laser pulse energy (solid line) compared to the concentration measured by pulsed-voltage APT (dashed line) and the nominal composition of the alloy (dotted line). Preferential evaporation of Ni is responsible for the inaccuracy in the concentrations measured by pulsed-laser and pulsed-voltage APT.

pulse energy. Interestingly, the alloy composition differs from both the nominal composition obtained by ICP chemical analysis, and the values measured by pulsed-voltage APT after the PLAP tomography runs at laser pulse energies of 0.6, 1.0, and 2.0 nJ. The compositions measured by pulsed-voltage APT were found to be 82.94 ± 0.08 Ni, 6.98 ± 0.02 Al, and 10.07 ± 0.03 Cr at.% and did not vary beyond experimental error. Even at the largest laser pulse energy, 2.0 nJ, the laser power has no cumulative, long-range effect on the tip composition.

The compositions measured by PLAP tomography are closer to the nominal composition of the alloy than those measured by pulsed-voltage APT of the same tip at 40 ± 0.3 K (Fig. 6). Previous studies of Ni-Al-Cr alloys by pulsed-voltage APT showed evidence of preferential field evaporation of Ni atoms resulting in differences between the expected and measured Ni concentration of 2.7 at.% for Ni-5.23 Al-14.77 Cr at.% (Schmuck et al., 1996), and 3.0 at.% for Ni-5.2 Al-14.2 Cr at.% (Sudbrack, 2004; Yoon, 2004; Sudbrack et al., 2006*b*, 2007; Booth-Morrison et al., 2008). These differences are greater than the 1.18 ± 0.08 at.% Ni measured here by pulsed-voltage APT. At a pulse energy of 0.6 nJ, the difference between the nominal Ni concentration and the value measured by PLAP tomography is 0.22 ± 0.14 at.%, suggesting that for the experimental conditions used herein, preferential evaporation is less severe in PLAP tomography than in voltage-pulsed APT, leading to improved compositional accuracy. The value of the effective pulse fraction at a laser pulse energy of 0.6 nJ per pulse is ~20%, which is close to the pulse fraction of ~19% that was determined to minimize preferential evaporation in Ni-Al-Cr systems in a pulsed-voltage APT (Schmuck et al., 1996; Sudbrack, 2004; Yoon, 2004). In both pulsed-voltage and PLAP tomography, the pulse fraction, or effective pulse fraction, respectively, has been recognized as the most important instrumentation parameter for controlling preferential evaporation; values of 15–20% are often cited as giving the most accurate compositional results (Bunton et al., 2007). In the case of PLAP tomography, an excessive effective pulse fraction can lead to overheating of the specimen tip, causing diffusion on the tip surface and resulting in a loss of spatial resolution (Kellogg & Tsong, 1980; Miller et al., 1996; Cerezo et al., 2007*b*).

The most striking feature of Figure 6 is the variation of the concentrations of the constituent elements with laser pulse energy during PLAP tomography. At laser pulse energies of 0.2–0.6 nJ, the measured Ni concentration increases, and the Al and Cr concentrations decrease, with increasing pulse energy. This suggests that the severity of Ni preferential evaporation decreases with increasing laser pulse energy, leading to a decrease in the detected concentration of solute atoms. At laser energies greater than 0.6 nJ per pulse, the Ni and Al concentrations do not vary beyond the experimental error. The measured Cr concentration increases with increasing pulse energy at energies of 1.0 nJ per pulse and greater. At a laser pulse energy of 2.0 nJ, the Cr concentration has increased by a statistically significant 0.11 ± 0.08 at.% Cr value over the value obtained for 0.6 nJ per pulse. The increase in the Cr concentration at 1.0 nJ per pulse and greater coincides with the evaporation of Cr^{1+} (Fig. 4). This effect cannot be ascribed to post-ionization but may be a result of a thermally activated evaporation mechanism for Cr^{1+}.

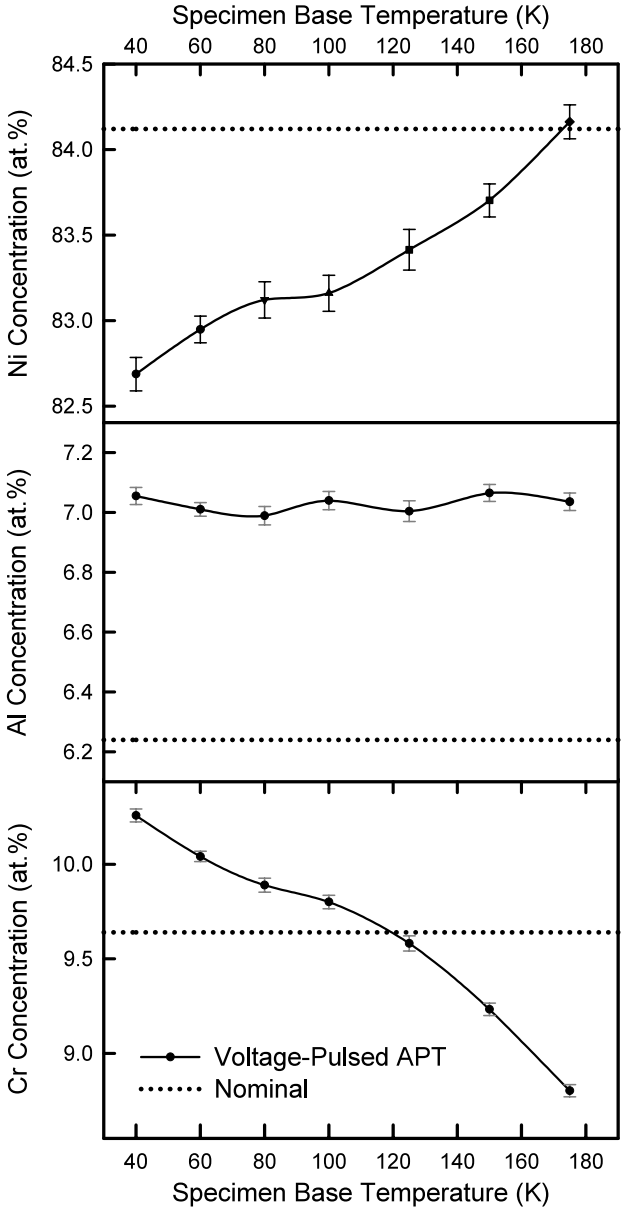

Figure 7. Variation of the detected composition of as-quenched Ni-6.5 Al-9.5 Cr at.% as a function of specimen base temperature by pulsed-voltage APT. At higher temperatures, preferential evaporation of Ni is less severe, while preferential evaporation of Cr is more severe.

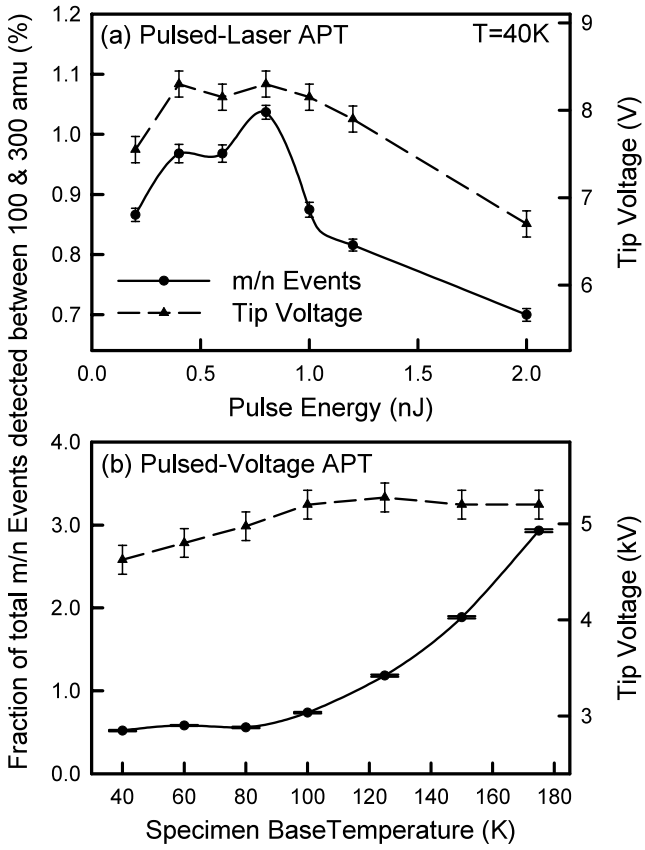

Figure 8. The relative frequency of detected events between 100–300 amu, as a function of (**a**) laser pulse energy in PLAP tomography and (**b**) specimen base temperature in pulsed-voltage APT. The amount of noise measured by PLAP tomography is directly proportional to the tip voltage and does not increase with increasing laser pulse energy, thus increasing thermal energy. On the contrary, the noise measured by pulsed-voltage APT increases as the specimen base temperature increases. This result demonstrates that the Ni-Al-Cr tips are not affected by significant steady-state heating during PLAP tomography.

Compositional Accuracy—Effects of Specimen Base Temperature

The effect of varying the specimen base temperature on the alloy composition measured by pulsed-voltage APT is displayed in Figure 7. The measured Ni concentration increases with increasing temperature, reaching the nominal composition at a temperature of 175 ± 0.3 K. Over the specimen base temperature range of 40–175 ± 0.3 K, the measured Al concentration remains constant, while the Cr concentration decreases by 1.43 ± 0.04 at.% Cr. As the specimen base temperature increases, and the tip voltage reaches a plateau value (Fig. 1a), and Ni preferential evaporation is diminished, while the preferential evaporation of Cr increases. This is a result of differences in the required evaporation fields of Ni and Cr at different temperatures.

Analysis of Events Detected at Mass-to-Charge State Ratios of 100–300 amu

An analysis of the events detected at m/n ratios between 100–300 amu, ranges where peaks are neither expected nor observed for this Ni-Al-Cr alloy, provides some insight into random field evaporation due exclusively to the steady-state dc tip voltage. Figure 8a shows that for PLAP tomography, the extent of random evaporation is directly proportional to the steady-state dc tip voltage and does not increase with

increasing pulse laser energy, and concomitantly increasing input thermal energy. The events detected in this same mass range for pulsed-voltage APT increase in frequency with increasing specimen base temperature (Fig. 8b) as a result of the decrease in the evaporation fields required for evaporation of the atomic species. This direct experimental result demonstrates clearly that results from PLAP tomography with picosecond laser pulsing for this Ni-Al-Cr alloy are not affected by significant steady-state heating of the tip. This is consistent with previous calculated estimates of the increase in tip temperature on the order of 200–300 K due to laser illumination (Kellogg, 1981*a*; Cerezo et al., 2006) and estimates of tip cooling times that are on the order of hundreds of nanoseconds (Lee et al., 1980).

The relative frequency of detected evaporation events with *m*/*n* ratios between 100–300 amu in the three pulsed-voltage APT measurements made between pulsed-laser analyses averaged 1.3 ± 0.1% of the total spectrum at an average tip voltage of 10.5 ± 1.0 kV. This should be compared to a value of 1.0 ± 0.1% of the total spectrum measured for the same tip, run by PLAP tomography at a steady-state dc voltage of 8.0–8.3 kV, for a laser energy of 0.6 nJ per pulse, and an equivalent pulse fraction of ~20%. Evaporation between pulses is less severe in PLAP tomography due to the lower steady-state dc voltage required to achieve a field evaporation rate of 0.04 ions per pulse, minimizing the preferential evaporation of Ni, as previously discussed.

Summary

The effects of picosecond laser pulse energy on the compositional accuracy and the quality of the mass spectra obtained for as-quenched Ni-6.5 Al-9.5 Cr at.% solid solutions analyzed by PLAP tomography are assessed. For the conditions used herein, it is found that when compared to pulsed-voltage APT, PLAP tomography yields improved mass resolving power and compositional accuracy and decreased noise levels. The most accurate compositional results are found at a laser pulse energy of 0.6 nJ per pulse, a specimen base temperature of 40 ± 0.3 K, a pulse repetition rate of 200 kHz, and a specimen evaporation rate of 0.04 ions per pulse; these conditions correspond to an effective pulse fraction of ~20%. An analysis of the events detected at *m*/*n* ratios of 100–300 amu by PLAP tomography with varying laser pulse energies shows no evidence for steady-state heating of the tips due to laser illumination.

The laser pulse energy is found to have an important impact on the observed *m*/*n* values of the evaporated species. The Ni^{1+}, Al^{1+}, and Cr^{1+} ions are observed to evaporate predominantly at higher laser energies, while at lower laser pulse energies, Ni^{2+}, Al^{2+}, and Cr^{2+} ions are predominantly detected, an effect that had previously been ascribed to post-ionization. The post-ionization model, however, is unable to account for (1) the decrease in the Ni^{2+}/Ni^{1+} and Al^{2+}/Al^{1+} ratios by more than two orders of magnitude when the laser energy is varied between 0.4–1.0 nJ per pulse at steady-state tip voltages ranging from 8.15–8.30 kV; (2) the detection of Ni^{1+} ions in pulsed-voltage APT exclusively at specimen base temperatures above 150 ± 0.3 K with a constant steady-state dc tip voltage. The latter indicates that the evaporation of Ni^{1+} occurs by a thermally activated process at higher temperatures, and thus it is unlikely that the evaporation of Ni^{2+}, Al^{2+}, and Cr^{2+} ions is due primarily to post-ionization of ions in the 1^+ charge state.

This study demonstrates the importance of selecting the correct instrumentation parameters to achieve compositional accuracy for a Ni-Al-Cr alloy, analyzed by either pulsed-laser and pulsed-voltage APT. A similar investigation is recommended for all materials systems, particularly those with small thermal diffusivities, prior to in-depth APT analysis to achieve optimal evaporation conditions and the highest degree of compositional accuracy.

Acknowledgments

This research was sponsored by the National Science Foundation (NSF) under grant DMR-0241928. Atom-probe tomographic measurements were performed at the Northwestern University Center for Atom-probe Tomography (NUCAPT). The LEAP™ tomograph was purchased with funding from the NSF-MRI (DMR 0420532, Dr. C. Bouldin, grant officer) and ONR-DURIP (N00014-0400798, Dr. J. Christodoulou, grant officer) programs and enhanced with a picosecond laser with funding from the ONR-DURIP (N00014-0610539, Dr. J. Christodoulou, grant officer). We thank Prof. T. Seideman for discussions and for providing additional references regarding tip heating under laser illumination, Dr. R. Noebe for sample preparation, and Prof. D. Isheim for managing NUCAPT. We extend our gratitude to the reviewers for their thoroughness and their helpful suggestions.

References

Bajikar, S.S., Larson, D.J., Kelly, T.F. & Camus, P.P. (1996). Magnification and mass resolution in local-electrode atom probes. *Ultramicroscopy* **65**(1–2), 119–129.

Booth-Morrison, C., Weninger, J., Sudbrack, C.K., Mao, Z., Noebe, R.D. & Seidman, D.N. (2008). Effects of solute concentrations on kinetic pathways in Ni-Al-Cr alloys. *Acta Mat* **56**(14), 3422–3438.

Brandon, D.G. (1964). The structure of field-evaporated surfaces. *Surf Sci* **3**, 1–18.

Brandon, D.G. (1965). The analysis of field evaporation data from field-ion microscope experiments. *Br J Appl Phys* **16**(5), 683–688.

Brandon, D.G. (1966*a*). Field evaporation. *Philos Mag* **14**(130), 803–820.

Brandon, D.G. (1966*b*). Field evaporation of dilute alloys. *Surf Sci* **5**(1), 137–146.

Bunton, J.H., Olson, J.D., Lenz, D.R. & Kelly, T.F. (2007). Advances in pulsed-laser atom probe: Instruments and specimen design for optimum performance. *Microsc Microanal* **13**, 418–427.

Cerezo, A., Clifton, P.H., Galtrey, M.J., Humphreys, C.J., Kelly, T.F., Larson, D.J., Lozano-Perez, S., Marquis, E.A., Oliver, R.A., Shab, G., Thompson, K., Zandbergen, M. & Alvis, R.L. (2007*a*). Atom probe tomography today. *Mater Today* **10**(12), 36–42.

Cerezo, A., Clifton, P.H., Gomberg, A. & Smith, G.D.W. (2007*b*). Aspects of the performance of a femtosecond laser-pulsed 3-dimensional atom probe. *Ultramicroscopy* **107**(9), 720–725.

Cerezo, A., Smith, G.D.W. & Clifton, P.H. (2006). Measurement of temperature rises in the femtosecond laser pulsed three-dimensional atom probe. *Appl Phys Lett* **88**(15), 154103/154101–154103/154103.

Ernst, N. (1979). Experimental investigation on field evaporation of singly and doubly charged rhodium. *Surf Sci* **87**(2), 469–482.

Forbes, R.G. (1976). A generalized theory of standard field ion appearance energies. *Surf Sci* **61**(1), 221–240.

Gault, B., Mottay, E., Courjaud, A., Vurpillot, F., Bostel, A., Menand, A. & Deconihout, B. (2007*a*). Ultrafast laser assisted field evaporation and atom probe tomography applications. *J Phys: Conf Ser* **59**, 132–135.

Gault, B., Vella, A., Vurpillot, F., Menand, A., Blavette, D. & Deconihout, B. (2007*b*). Optical and thermal processes involved in ultrafast laser pulse interaction with a field emitter. *Ultramicroscopy* **107**(9), 713–719.

Gerstner, V., Thon, A. & Pfeiffer, W. (2000). Thermal effects in pulsed laser assisted scanning tunneling microscopy. *J Appl Phys* **87**(5), 2574–2580.

Gomer, R. (1959). Field desorption. *J Chem Phys* **31**, 341–345.

Gomer, R. (1961). *Field Emission and Field Ionization*. Cambridge, MA: Harvard University Press.

Gomer, R. & Swanson, L.W. (1963). Theory of field desorption. *J Chem Phys* **38**, 1613–1629.

Grafstrom, S. (2002). Photoassisted scanning tunneling microscopy. *J Appl Phys* **91**(4), 1717–1753.

Hall, T.M., Wagner, A. & Seidman, D.N. (1977). A computer-controlled time-of-flight atom-probe field-ion microscope for the study of defects in metals. *J Phys E* **10**(9), 884–893.

Haydock, R. & Kingham, D.R. (1980). Post-ionization of field-evaporated ions. *Phys Rev Lett* **44**(23), 1520–1523.

Herschitz, R. & Seidman, D.N. (1983). A quantitative atom-probe field-ion microscope study of the compositions of dilute cobalt-niobium and cobalt-iron alloys. *Surf Sci* **130**(1), 63–88.

Kellogg, G.L. (1981*a*). Determining the field emitter temperature during laser irradiation in the pulsed laser atom probe. *J Appl Phys* **52**(8), 5320–5328.

Kellogg, G.L. (1981*b*). Experimental evidence for multiple post-ionization of field-evaporated ions. *Phys Rev B* **24**(4), 1848–1851.

Kellogg, G.L. (1982). Measurement of the charge state distribution of field evaporated ions: Evidence for post-ionization. *Surf Sci* **120**(2), 319–333.

Kellogg, G.L. (1987). Pulsed-laser atom probe mass spectroscopy. *J Phys E* **20**(2), 125–136.

Kellogg, G.L. & Tsong, T.T. (1980). Pulsed-laser atom-probe field-ion microscopy. *J Appl Phys* **51**(2), 1184–1193.

Kelly, T.F., Camus, P.P., Larson, D.J., Holzman, L.M. & Bajikar, S.S. (1996). On the many advantages of local-electrode atom probes. *Ultramicroscopy* **62**(1–2), 29–42.

Kelly, T.F. & Larson, D.J. (2000). Local electrode atom probes. *Mater Charact* **44**(1/2), 59–85.

Kelly, T.F., Larson, D.J., Thompson, K., Alvis, R.L., Bunton, J.H., Olson, J.D. & Gorman, B.P. (2007). Atom probe tomography of electronic materials. *Annu Rev Mater Res* **37**, 681–727.

Kelly, T.F. & Miller, M.K. (2007). Invited review article: Atom probe tomography. *Rev Sci Instrum* **78**(3), 031101/031101–031101/031120.

Kingham, D.R. (1982). The post-ionization of field evaporated ions: A theoretical explanation of multiple charge states. *Surf Sci* **116**(2), 273–301.

Larson, D.J., Petford-Long, A.K., Ma, Y.Q. & Cerezo, A. (2004). Information storage materials: Nanoscale characterisation by three-dimensional atom probe analysis. *Acta Mat* **52**(10), 2847–2862.

Lee, M.J.G., Reifenberger, R., Robins, E.S. & Lindenmayr, H.G. (1980). Thermally enhanced field emission from a laser-illuminated tungsten tip: Temperature rise of tip. *J Appl Phys* **51**(9), 4996–5006.

Miller, M.K., Cerezo, A., Hetherington, M.G. & Smith, G.D.W. (1996). *Atom Probe Field Ion Microscopy*. Oxford: Clarendon Press.

Miller, M.K. & Smith, G.D.W. (1989). *Atom Probe Microanalysis: Principles and Applications to Materials Problems*. Pittsburgh, PA: MRS.

Müller, E.W. (1956). Field desorption. *Phys Rev* **102**, 618–624.

Müller, E.W. & Krishnaswamy, S.V. (1976). High ionic charges in field-evaporating 5d transition metals. *Phys Rev Lett* **37**(15), 1011–1014.

Müller, E.W. & Tsong, T.T. (1969). *Field Ion Microscopy*. New York: American Elsevier Publishing Company.

Nakamura, S. & Kuroda, T. (1977). Ionization states of ions field-evaporated from the refractory metal alloys. *Jpn J Appl Phys* **16**(8), 1499–1500.

Parratt, L.G. (1966). *Probability and Experimental Errors in Science*. New York: John Wiley.

Schmuck, C., Danoix, F., Caron, P., Hauet, A. & Blavette, D. (1996). Atomic scale investigation of ordering and precipitation processes in a model Ni-Cr-Al alloy. *Appl Surf Sci* **94–5**, 273–279.

Seidman, D.N. (2007*a*). Perspective: From field-ion microscopy of single atoms to atom-probe tomography: A journey. *Rev Sci Instrum* **78**(3), 030901/030901–030901/030903.

Seidman, D.N. (2007*b*). Three-dimensional atom-probe tomography: Advances and applications. *Annu Rev Mater Res* **37**, 127–158.

Smith, G.D.W., Grovenor, C.R.M., Delargy, K.M., Godfrey, T.J. & McCabe, A.R. (1982). Direct comparison of performance of atom probe in pulsed-laser and voltage-pulsed modes. *IFES Proc* 283–289.

Southon, M.J. (1968). Field emission and field ionization. In *Field-Ion Microscopy*, Hren, J.J. & Ranganathan, S. (Eds.), pp. 6–27. New York: Plenum Press.

Sudbrack, C.K. (2004). Ph.D. Thesis. *Decomposition Behavior in Model Nickel-Aluminum-Chromium-X Superalloys: Temporal Evolution and Compositional Pathways on a Nanoscale*. Evanston, IL: Northwestern University.

Sudbrack, C.K., Noebe, R.D. & Seidman, D.N. (2006*a*). Direct observations of nucleation in a nondilute multicomponent alloy. *Phys Rev B* **73**(21), 212101/212101–212101/212104.

Sudbrack, C.K., Noebe, R.D. & Seidman, D.N. (2007). Compositional pathways and capillary effects during early-stage isother-

mal precipitation in a nondilute Ni-Al-Cr alloy. *Acta Mat* **55**, 119–130.

Sudbrack, C.K., Yoon, K.E., Noebe, R.D. & Seidman, D.N. (2006*b*). Temporal evolution of the nanostructure and phase compositions in a model Ni-Al-Cr alloy. *Acta Mat* **54**(12), 3199–3210.

Tsong, T.T. (1978). Field ion image formation. *Surf Sci* **70**, 211–233.

Tsong, T.T. (1990). *Atom-Probe Field Ion Microscopy*. Cambridge, UK: Cambridge University Press.

Tsong, T.T. & Müller, E.W. (1970). Field evaporation rates of tungsten. *Phys Stat Sol A* **1**(3), 513–533.

Vella, A., Vurpillot, F., Gault, B., Menand, A. & Deconihout, B. (2006). Evidence of field evaporation assisted by nonlinear optical rectification induced by ultrafast laser. *Phys Rev B* **73**(16), [165416/165411–165416/165417].

Vurpillot, F., Gault, B., Vella, A., Bouet, M. & Deconihout, B. (2006). Estimation of the cooling times for a metallic tip under laser illumination. *Appl Phys Lett* **88**(9), [094105/094101–094105/094103].

Wada, M. (1984). On the thermally activated field evaporation of surface atoms. *Surf Sci* **145**(2–3), 451–465.

Yamamoto, M. & Seidman, D.N. (1982). Quantitative compositional analyses of ordered platinum-cobalt (Pt_3Co) by atom-probe field-ion microscopy. *Surf Sci* **118**(3), 535–554.

Yamamoto, M. & Seidman, D.N. (1983). The quantitative compositional analysis and field-evaporation behavior of ordered nickel-molybdenum (Ni_4Mo) on an atomic plane-by-plane basis: An atom-probe field-ion microscope study. *Surf Sci* **129**(2–3), 281–300.

Yoon, K.E. (2004). Ph.D. Thesis. *Temporal Evolution of the Chemistry and Nanostructure of Multicomponent Model Nickel-Based Superalloys*. Evanston, IL: Northwestern University.

Zemansky, M.W. (1957). *Heat and Thermodynamics*, 4th ed., pp. 326–327. New York: McGraw-Hill Book Company.